Research Square

Preprints are preliminary reports that have not undergone peer review.
They should not be considered conclusive, used to inform clinical practice,
or referenced by the media as validated information.

Interaction-driven modification of agar-based biodegradable films using Carpobrotus glaucescens phytochemical extracts

Rishi Ravindra Naik

r.naik@unsw.edu.au

UNSW Sydney

Que Trinh Tran

UNSW Sydney

Muhammad Bin Zia

UNSW Sydney

Cordelia Selomulya

UNSW Sydney

Research Article

Keywords: Agar film, phytochemical extract, concentration-dependent behaviour, polyphenols, biodegradable materials, moisture sensitivity

Posted Date: May 6th, 2026

DOI: https://doi.org/10.21203/rs.3.rs-9453943/v1

License: This work is licensed under a Creative Commons Attribution 4.0 International License.
Read Full License

Additional Declarations: No competing interests reported.

Version of Record: A version of this preprint was published at Journal of Polymers and the Environment on October 16th, 2026. See the published version at https://doi.org/10.1007/s10924-026-04015-x.

Interaction-driven modification of agar-based biodegradable films using *Carpobrotus glaucescens* phytochemical extracts

Rishi Ravindra Naik*, Que Trinh Tran, Muhammad Bin Zia, Cordelia Selomulya

School of Chemical Engineering, UNSW Sydney, Kensington, NSW 2052, Australia.

Correspondence details:

*r.naik@unsw.edu.au

Abstract

Agar-based films are promising biodegradable materials, but their inherent brittleness and high moisture sensitivity limit practical use. In this study, a phytochemical extract from the Australian halophyte *Carpobrotus glaucescens* was investigated as a modifier of agar films, based on its richness in hydroxyl-functionalised polyphenols and low-molecular-weight carbohydrates that can interact with polysaccharide chains and influence network structure. Chemical characterisation (CHNS, FT-IR, ^{1}H NMR and LC-MS) confirmed the presence of these hydroxyl-rich constituents capable of intermolecular interactions with agar. Incorporation of the extract significantly altered film behaviour; at an agar-to-extract ratio of 1:20 (w/v), tensile strength increased by 38% and elongation at break increased to 23% relative to the control, while water vapour permeability decreased from 2.91×10^{-11} to 1.26×10^{-11} g/m²·s·Pa ($p < 0.05$). These improvements were associated with a denser microstructure and enhanced network cohesion. At higher extract loadings, aggregation of phytochemical constituents disrupted matrix continuity and reduced mechanical performance, indicating a non-linear response governed by the balance between intermolecular interactions and phase separation. At intermediate levels, hydrogen bonding and increased chain mobility produced a more cohesive and flexible network, while excessive loading led to self-association and structural discontinuities. Despite these improvements, the films remained highly water-soluble due to the hydrophilic nature of the system. These findings demonstrate that phytochemical extracts act as concentration-dependent modifiers rather than linear additives, defining a compositional window for optimising structure-property relationships in bio-based polymer films.

Keywords:

Agar film; phytochemical extract; concentration-dependent behaviour; polyphenols; biodegradable materials; moisture sensitivity

1. Introduction

Polysaccharide-based films fabricated from agar have attracted considerable attention as biodegradable alternatives to conventional plastics due to their renewable nature, film-forming ability, and transparency [1]. However, native agar films are inherently brittle, exhibiting limited flexibility and poor water-barrier performance, which restrict their practical application. The incorporation of plasticisers is therefore necessary to improve polymer chain mobility and functional properties, although current approaches predominantly rely on purified low-molecular-weight compounds. The development of alternative plasticising systems is particularly relevant in the context of escalating plastic pollution, with global plastic production exceeding 450 million tonnes annually [2]. Conventional plastics, including polyethylene, polypropylene, polyesters, polyvinyl chloride, and polyamides, are derived from fossil hydrocarbons and are widely used in single-use applications but their non-degradable nature contributes to persistent environmental contamination [3, 4]. In response, biodegradable films formulated from biopolymers such as agar or starch have been proposed as sustainable alternatives; however, their performance remains dependent on the incorporation of effective modifiers.

Recent studies [5-8] have explored the use of plant-derived compounds as plasticising agents; however, these investigations have focused on isolated molecules rather than complex phytochemical mixtures. Several individual phytochemicals, including trehalose, digeneaside, and glucose, have been directly incorporated into biodegradable film systems to act as plasticisers in these studies. While these studies demonstrate the effectiveness of specific compounds, they do not capture the potential synergistic effects of intact phytochemical matrices, which contain diverse polyphenols, carbohydrates, and organic acids. As a result, the structural and functional role of whole plant-derived phytochemical mixtures in polysaccharide-based film systems remains underexplored.

In Australia, bush foods represent a diverse group of native plant resources traditionally used by Indigenous communities for nutritional, medicinal, and cultural purposes [9]. Despite the presence of more than 26,000 native plant species, many remain underutilised due to seasonal variability, lack of characterisation / understanding of their properties, and limited collaboration frameworks [10, 11]. *Carpobrotus glaucescens*, commonly known as pigface or ice plant, represents one such native species. Belonging to the family *Aizoaceae*, it grows on coastal sand dunes from Mackay in Queensland to eastern Victoria [12]. Phytochemical evidence from a related species, *Carpobrotus edulis*, demonstrates the presence of diverse compounds including peptides, saccharides and polyphenols [13]. As a halophyte adapted to saline and oxidative stress environments, *C. glaucescens* is likely to accumulate stress-associated metabolites, including polyphenols and soluble carbohydrates, which are rich in hydroxyl and carboxyl functionalities capable of interacting with polysaccharide networks.

In this study, the phytochemical profile of *Carpobrotus glaucescens* was characterised with particular focus on its polyphenolic and carbohydrate constituents due to their high density of functional groups and their potential to participate in intermolecular interactions. It was hypothesised that pigface-derived phytochemical mixtures would act as active modifiers rather than inert fillers, as previous studies have shown that low-molecular-weight compounds such as sugars can function as plasticising agents in polysaccharide-based films [5-8]. Extending this concept to chemically complex plant extracts containing both carbohydrates and polyphenols, these mixtures were expected to alter agar network behaviour through concentration-dependent interactions..

2. Materials and methods

2.1. Materials

Pigface (*Carpobrotus glaucescens*) leaves were sourced from IndigiGrow Community Nursery, and Bush to Bowl nursery, (Australia). *Gracilaria secundata* (GS) was obtained from Meron-Marine Hydrocolloids (India). All chemicals used were of analytical grade and were purchased from Chemsupply (Australia) and Sigma-Aldrich (Australia).

2.2. Freeze dried-powder characterization

Fresh pigface leaves were freeze-dried (CD8 CryoDry, Australia) for 48 hours, ground and stored in a desiccator at room temperature. The colour (L*=61.6 ± 0.42, a*=-5.73 ± 0.29, b*=13.24 ± 0.56) of the dried powders was measured using a handheld colourimeter (CHNSpec, China). The elemental analysis for C, H, N and S was carried out following a method by Elementar Analysensysteme GmbH [14]. Approximately 20-200 mg of freeze-dried powder was weighed in tin foil capsules and combusted at 1150 °C. The resulting gases were analysed for elemental quantification.

2.2.1. Amino acid analysis

Amino acids were quantified following acid hydrolysis (6 M HCl, 110 °C, 24 h) using established protocols [15-18]. Hydrolysates were derivatised with 6-aminoquinolyl-N-hydroxysuccinimidyl carbamate and analysed using an ACQUITY UPLC system with UV detection (Waters) and an AccQ•Tag Ultra BEH C18 column (2.1 × 100 mm, 1.7 μm) at 57 °C. Detection was performed at 260 nm with a 0.7 mL min^{-1} flow rate. Tryptophan and cysteine were not quantified due to acid sensitivity.

2.2.2. Spectroscopic analysis (FT-IR and 1H-NMR)

The FTIR spectrum were recorded using Bruker Alpha (Bruker, USA) with a universal attenuated total reflectance accessory (ATR platinum diamond), following the method described by Lv et al. [19] . Briefly, the spectra were recorded from 400-4000 cm^{-1} with a resolution of 2 cm^{-1} (32 scans). Baseline correction was performed using Bruker OPUS software (version 6.5) and visualised using Spectragryph software (version 1.2.16.1).

The NMR spectra was measured as described by Kim et al. [20]. Briefly, 50mg freeze-dried powders were mixed with 0.75 ml of CH_3OH-d4 and 0.75 ml of KH_2PO_4 buffer in D_2O (pH 6.0) containing 0.1% (w/w) 3-trimethylsilyl propionic 2,2,3,3-d4 acid (TSP) as an internal standard. Samples were vortexed for 1 minute, sonicated for 15 minutes at room temperature (20-25 °C) and centrifuged at 6,000 rpm for 10 minutes. The supernatants were analysed using 1H-NMR spectrometer (Weber 400 MHz), spectra processed using Bruker TopSpin version 4.0 followed by library search using Colmar 1D (https://colmar.cloud/index.php/colmar) and BMRB database (https://bmrb.io/).

2.2.3. Metabolomics and elemental analysis (LC-MS and ICP-MS)

Untargeted metabolomics was performed using an UltiMate 3000 UHPLC system coupled to a Q Exactive HF Orbitrap mass spectrometer (Thermo Fisher Scientific). Freeze-dried powder was extracted in acetonitrile: methanol: formic acid (80:20:0.1, v/v/v), sonicated, and centrifuged. Supernatants were analysed using C18 and HILIC separations with electrospray ionisation (HESI-II source). Full MS scans (m/z 100-1500) were acquired at high resolution, followed by data-dependent MS/MS.

Trace elements were quantified by ICP-MS following microwave-assisted digestion [21]. Approximately 0.5 g powder was digested in HNO_3/HCl using an Ethos 1 system (Milestone, Italy). Analyses were performed using a NexION® 5000 ICP-MS (PerkinElmer, USA).

2.2.4. Antioxidant assays

Total phenolic content (TPC), DPPH radical scavenging and Trolox equivalent antioxidant capacity (TEAC) was measured according to a method by Bobo-García et al. [22] with gallic acid (TPC), Trolox (DPPH) as a standard and total flavonoid content (TFC) assay was measured according to a method by Sari et al. [23] using quercetin as standard.

2.3. Film preparation and characterisation

2.3.1. Agar extraction

Agar was extracted from *Gracilaria secundata* powder following the method Martínez-Sanz et al. [24] with modifications. Briefly, 30 g of powder was dispersed in 1 L Milli-Q water and heated at 90 °C for 2 h. The hot extract was filtered, subjected to two freeze-thaw cycles, freeze-dried (CD8-CryoDry, Australia), and stored in a desiccator at ambient temperature until use. Agar obtained from *Gracilaria spp*. is composed primarily of agarose and agaropectin fractions, which are responsible for its gel-forming and film-forming behaviour. The selected extraction conditions were chosen based on established protocols known to yield agar with physicochemical characteristics suitable for film applications, where extraction temperature and duration influence polysaccharide structure and functionality.

2.3.2. Extraction of bioactives from pigface

Bioactive components from pigface leaves were extracted using the method specified by Ermi Hikmawanti et al. [25]. Freeze-dried powder was extracted with 50% (v/v) ethanol at a 1:10 ratio for 3 h at 25 °C. Extracts were filtered and concentrated using a rotary evaporator (Across International, Australia) at 50 °C.

2.3.3. Preparation of composite films

A central composite design (CCD) was employed to systematically evaluate the effect of agar-to-pigface extract ratio (A:PF w/v) on film properties and to identify the optimal formulation (Supplementary Table 1). Agar and pigface extracts were mixed and stirred at 45 °C for 1 h, centrifuged (6000 rpm, 3 min), and the supernatant was cast onto acrylic Petri dishes (85 mm diameter). Films were dried at 40 °C for 4 h in a dehydrator and stored at 25 °C in a desiccator prior to analysis.

2.3.4. Particle size and zeta potential

The particle size and zeta potential of different film-forming solutions were measured before and after centrifugation at 6,000 rpm for 3 minutes using a Zetasizer (Malvern Instruments, UK) to assess dispersion stability and potential interactions between agar and pigface derived components in the film-forming solutions.

2.3.5. Optical properties and microstructure

Film colour (L*, a*, b*) and opacity were measured using a calibrated colourimeter (CHNSpec, China). Film thickness was determined using a digital micrometer (average of 10 measurements per film). Microstructure was examined using optical microscopy (Nikon Eclipse Ci-L, 40× magnification).

2.3.6. Mechanical properties

Tensile strength and elongation at break were measured using a Texture Analyser (TA-XTplus texture analyser, USA) in accordance with ASTMD882-02 [26]. The films were cut into strips (26×10 mm), with thicknesses ranging from 15-20 μm. All measurements were performed in triplicate, and the results were reported as mean values.

2.3.7. Moisture content and water solubility

The moisture content (MC) of the film was measured using the method described by Homez-Jara et al. [27]. Briefly, the films specimens (20 × 20 mm) were weighed to obtain the initial mass (M_0) and dried at 105 °C for 24 hours to obtain the dry mass (M_1). The dried films were immersed in 50 mL of Milli-Q water at ambient temperature for 24 hours and the insoluble residues were collected by vacuum filtration and redried to obtain the final mass (M_2). Moisture content and water solubility (%) were calculated as follows:

$$\%\, Moisture\ content = \left(\frac{M_0 - M_1}{M_0}\right) * 100 \quad (1)$$

$$\%\, Water\ solubility = \left(\frac{M_1 - M_2}{M_1}\right) * 100 \quad (2)$$

2.3.8. Water vapour permeability (WVP)

Water vapour permeability (WVP) was determined using the ASTM E96-95 gravimetric method described by Sutharsan et al. [28]. Film samples were sealed over the opening of centrifuge tubes (15 mm diameter) containing 7.7 g of silica gel. The assemblies were weighed and stored at 23 °C and 60% relative humidity. Weight gain was recorded over time, and the water vapour transmission rate (WVTR) was calculated from the slope of weight gain versus time. WVP was calculated using:

$$WVP = \frac{WVTR * L}{p} \quad (3)$$

Where L is the thickness of the film and P is the partial pressure at 23 °C

2.3.9. Contact angle

Surface wettability was evaluated by contact angle measurements using a sessile drop method with an Attension Theta Lite optical tensiometer (Biolin Scientific, Sweden). A 4 µL droplet of Milli-Q water was deposited onto the film surface, and images were recorded for 30 s. The contact angle was determined using OneAttension software, and values are reported as the mean of ten measurements.

2.3.10. Antioxidant properties

Film extracts were prepared as reported by Makhloufi et al. [29]. Total phenolic content (TPC), DPPH radical scavenging activity, and Trolox equivalent antioxidant capacity (TEAC) were determined as described by Bobo-García et al. [22]. DPPH scavenging activity was calculated using:

$$\%\ \text{DPPH quenched} = \left[1 - \left(\frac{As - Ab}{Ac - Ab}\right)\right] * 100 \quad (4)$$

Where *As, Ab* and *Ac* are the absorbances of samples, blank and control.

2.4. Data Analysis

Data were analysed using one-way analysis of variance (ANOVA). Results are presented as mean ± standard deviation. Statistical significance was determined at $p < 0.05$.

3. Results & Discussion

3.1. Pigface extract characterization

3.1.1. CHNS and Amino acid analysis

CHNS analysis (Supplementary table 2) of the pigface samples showed low sulphur content (0.27 ± 0.05 %) and a relatively high C/N ratio (29.34 ± 0.77/3.69 ± 0.12) indicating a low contribution of proteinaceous components, suggesting that interactions within the agar matrix are unlikely to be driven by protein-polysaccharide complexation or sulphur-mediated crosslinking. Instead, the elevated C/N ratio reflects a predominance of carbon-rich secondary metabolites, including polyphenols and carbohydrates, which are characterised by multiple hydroxyl functionalities and is consistent with a capacity for hydrogen bonding and secondary intermolecular interactions with agar chains [30] and is discussed further in section 3.1.6.

Pigface contained approximately 6% protein on a dry weight basis, representing a minor component relative to polysaccharide and polyphenol fractions. The amino acid profile was dominated by acidic residues, particularly glutamic (133.7 mg/g protein) and aspartic acid (100.7 mg/g protein), along with appreciable levels of polar and aliphatic amino acids such as lysine (72.6 mg/g protein), leucine (90.8 mg/g protein), and valine (62.7 mg/g protein). This distribution indicates the presence of carboxyl, amine, and hydroxyl functionalities, which may contribute to secondary interactions within the agar matrix through hydrogen bonding and electrostatic associations [6]. However, given the low overall protein content, nitrogenous compounds are expected to play a secondary role in network modification and are unlikely to act as primary structural determinants in the film system.

3.1.2. Spectroscopic characterization (FT-IR and 1H-NMR)

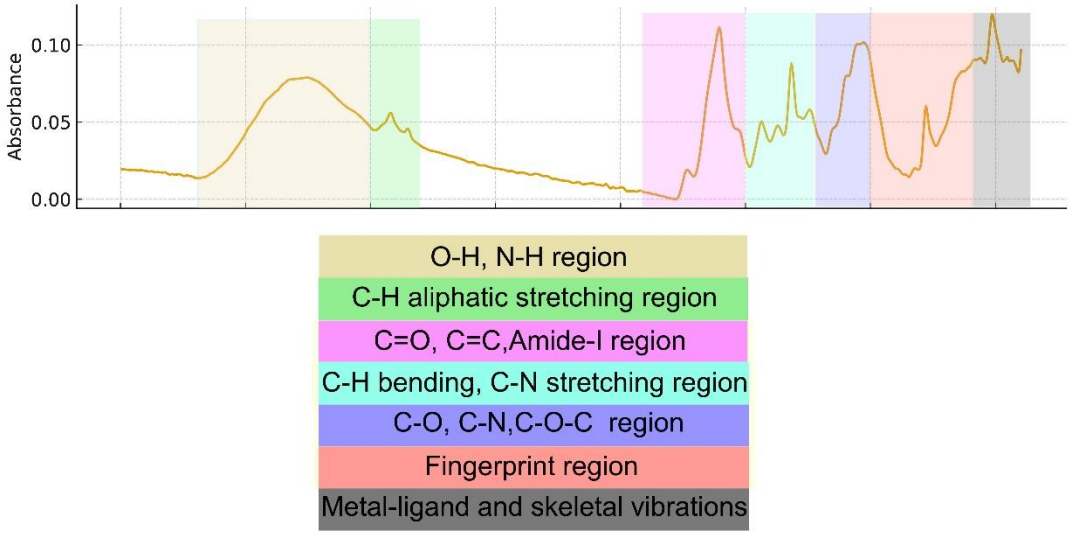


Fig. 1 FT-IR spectrum of pigface powder showing major functional groups

Fourier-transform infrared (FT-IR) spectroscopy (Figure 1) revealed a broad absorption band at 3200-3600 cm^{-1} corresponding to O-H stretching, indicating abundant hydrogen-bonded hydroxyl groups consistent with polyphenols and polyols [31]. Strong bands in the range 1000-1200 cm^{-1} were assigned to C-O and C-O-C stretching, characteristic of polysaccharides and glycosidic linkages. A peak near 1640 cm^{-1} was attributed to C=O stretching and/or aromatic C=C vibrations, with a weaker shoulder around 1540 cm^{-1} suggesting contributions from amide groups and conjugated aromatic structures [32].

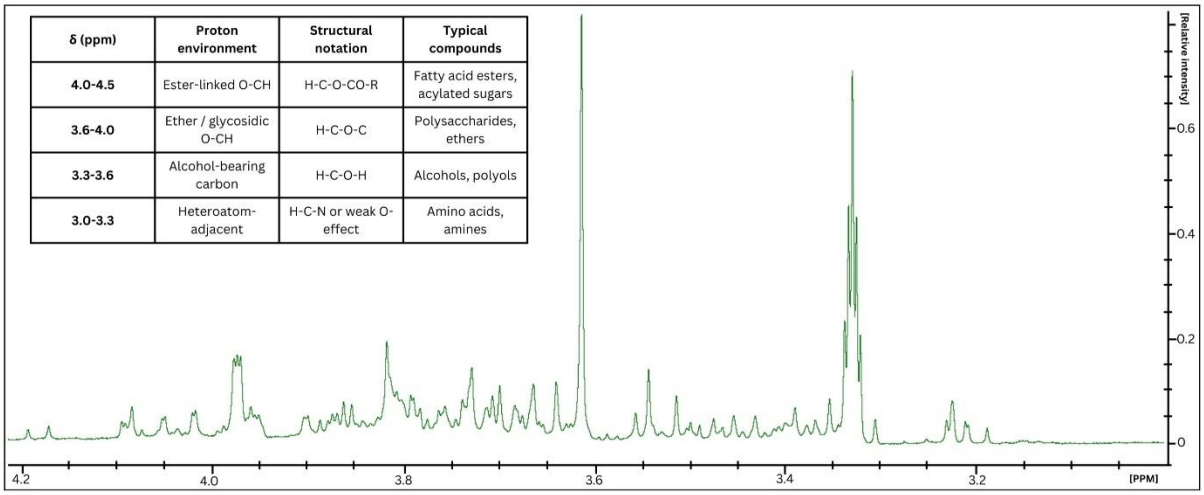


Fig. 2 ^{1}H NMR spectrum of freeze-dried pigface with corresponding chemical shift assignments adapted from Seo [66]

^{1}H NMR spectra (Figure 2), referenced to TSP (δ = 0 ppm) [20], were dominated by signals between δ 3.2 and 4.2 ppm, corresponding to protons adjacent to electronegative atoms, particularly oxygen. The presence of overlapping multiplets in this region is consistent with O-CH and O-CH_2 environments typical of carbohydrates, polyols, and glycosidic structures. The absence of significant downfield signals beyond δ 4.1 ppm indicates a limited contribution from esterified or aromatic proton environments, confirming that the extract is predominantly composed of oxygenated aliphatic compounds [33]. These features support the presence of hydroxyl-rich constituents capable of participating in intermolecular interactions with agar chains.

3.1.3. Metabolomics (LC-MS) and elemental analysis (ICP-MS)

LC-MS profiling revealed a phytochemical fingerprint characteristic of *Carpobrotus spp.* (Figure 3), dominated by polyphenols (Figure 6(d)) including phenolic acids. The identified metabolites included chlorogenic/p-coumaroylquinic, ferulic acid and flavonoids including catechin, taxifolin, quercetin, and phlorizin. These compound classes are widely reported in *Carpobrotus spp.* and other *Aizoaceae* succulents and support the plant's antioxidant activity and traditional medicinal use [34]. Caffeoyl-/coumaroyl-quinic acid derivatives were the prominent phenylpropanoid esters, while flavonol glycosides were the most abundant flavonoid subclass.

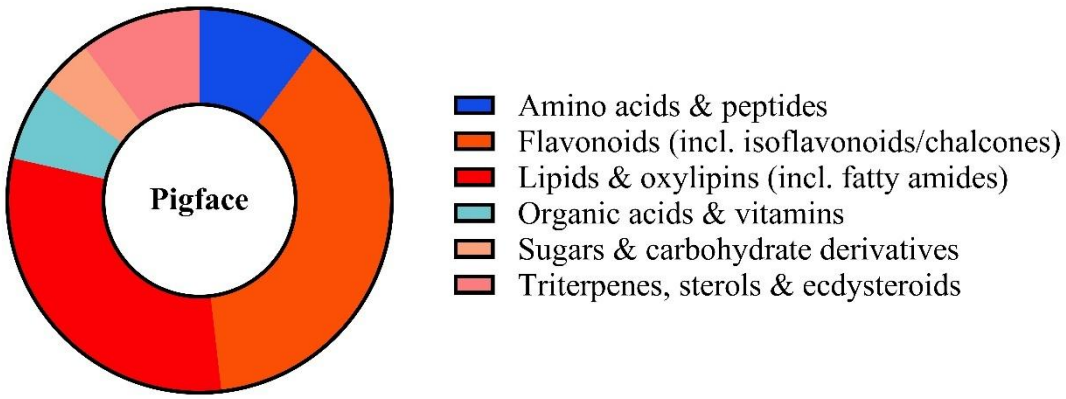


Fig. 3 Distribution of phytochemical classes in pigface extract based on compound counts

In addition to polyphenols, primary metabolites including ascorbate, quinic acid, trehalose, and D-pinitol, along with soluble carbohydrates such as fructose and sucrose, were detected. The presence of these low-molecular-

weight compounds is consistent with a chemically diverse extract capable of influencing polymer network behaviour.

ICP-MS analysis indicated the presence of trace elements, including arsenic (14.35 mg/kg), cadmium (0.07 mg/kg), lead (0.2 mg/kg), and mercury (0.007 mg/kg). Mercury levels were below the Codex limit of 0.1 mg/kg, indicating no immediate concern [35]. The elevated arsenic content is likely associated with environmental uptake in coastal and saline conditions, where metalloid mobility can be enhanced [36]. Saline, sandy coastal substrates may further enhance metalloid mobility and thus could be a contributing factor of high levels of arsenic [37]. This indicates the potential of pigface plant to act as an accumulator of arsenic, although targeted accumulation studies are required to confirm this hypothesis while also highlighting the importance of raw material sourcing when considering plant-derived additives for material applications. Trace elemental composition of the films was also evaluated by ICP-MS (Supplementary Table 6). Low concentrations of Cd and Hg were detected in the oprimized sample P5, while arsenic was present at higher levels in films containing pigface extract, reflecting its presence in the raw material. Incorporation into the agar matrix reduced the overall concentration relative to the extract due to dilution effects. Although these elements did not influence the physicochemical properties assessed in this study, their presence highlights the importance of raw material sourcing and contaminant monitoring when considering plant-derived additives for material applications.

3.1.4. Antioxidant activity

Pigface exhibited strong antioxidant activity, consistent with its phenolic composition. The total phenolic content (TPC) was 27.45 ± 0.41 mg GAE/g and total flavonoid content (TFC) was 2.42 ± 0.30 mg QE/g, corresponding with its antioxidant capacity measured by DPPH (TEAC: 7.03 ± 0.03 mg Trolox/g) and ferric reducing antioxidant power (FRAP: 2.59 ± 0.33 μmol Fe^{2+}/g). These values are consistent with previous reports for *Carpobrotus species*; for example, Akinyede et al. [38] reported a TFC of 1.19 ± 0.04 mg QE/g in *Carpobrotus edulis*, supporting the role of phenolic compounds in driving antioxidant activity.

This behaviour is consistent with the structural and compositional analyses presented earlier. FT-IR and NMR results indicated the presence of hydroxyl-rich and oxygenated functional groups, while LC-MS profiling identified phenolic acids, flavonoids, and other redox-active metabolites such as ascorbate. These compounds are known to contribute to antioxidant activity through hydrogen atom donation and electron transfer mechanisms.

3.2. Characterisation of films

3.2.1. Particle size and zeta potential

Particle size analysis was conducted to evaluate dispersion behaviour and the effect of centrifugation on the removal of larger aggregates. The raw pigface extract exhibited an average particle size of 1.25 ± 0.26 μm, whereas agar alone showed a larger size of 3.43 ± 1.39 μm. Upon incorporation into agar, the average particle size of the film-forming solutions increased to 6.67 ± 1.06 μm at lower extract concentrations, suggesting the formation of aggregated structures. This behaviour is consistent with polyphenol-polysaccharide interactions that promote association through hydrogen bonding and hydrophobic interactions [39]. In contrast, the formulation with higher pigface content (P9) exhibited a smaller average particle size (1.27 ± 1.18 μm), indicating a change in dispersion behaviour at elevated extract concentrations. Centrifugation had minimal effect on P9, whereas in intermediate formulations (e.g., P6), particle size decreased after centrifugation, suggesting sedimentation of larger agar-pigface aggregates.

Zeta potential measurements showed that agar exhibited a higher negative surface charge (−27.64 ± 2.30 mV) compared to the pigface extract (−6.95 ± 0.45 mV), while composite systems displayed intermediate values (−17.45 ± 1.42 mV), indicating interaction between the two components. Although the reduction in ζ-potential magnitude suggests partial charge neutralisation, the values were insufficient to ensure strong electrostatic stabilisation, supporting the observed tendency toward aggregation at higher extract concentrations [40]. Overall,

the particle size and zeta potential data indicate that pigface extract concentration influenced dispersion behaviour and particle association in the film-forming solutions, which is consistent with the observed differences in film microstructure and mechanical performance.

3.2.2. Optical properties and microstructure

Agar is a seaweed-derived polysaccharide composed of 1,3-linked β-D-galactopyranose and 1,4-linked 3,6-anhydro-α-L-galactopyranose units that forms a gelatinous network in aqueous systems [41]. The appearance of composite films is presented in Figure 4, which shows smooth surfaces and were generally transparent with a pale-yellow hue. Increasing the pigface extract concentration beyond A:PF of 1:40 (w/v) reduced its transparency and intensified the yellow coloration, which is attributed to the higher polyphenol content of pigface (Figure 6(d)) and corresponds to an increased CIELab b* value ($p<0.05$) reflecting yellowness. Similar trend was reported by Wang et al. [42] wherein the tea polyphenols were incorporated into chitosan film and by Sun et al. [43] via addition of apple polyphenols to chitosan-based films.

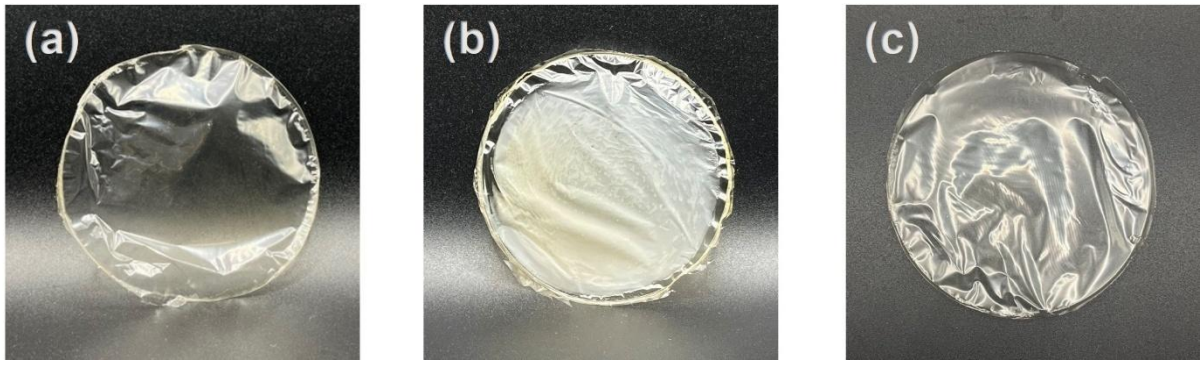


Fig. 4 Concentration-dependent colour changes in agar films incorporating pigface extract: (a) A:PF 1:20 (P6); (b) A:PF 1:40 (P9); (c) control agar film

Color parameters, including lightness (L*), a* (red-green), and b* (yellow-blue) and opacity (%) are shown in Figure 5. Film lightness ranged from 88.10 ± 1.84, with only the highest pigface formulation (1:40 w/v) showing significant decrease in L* compared to other films. Film transparency is a desirable packaging trait for product appearance [44] and a higher opacity indicates lower transparency. The a* values remained statistically unchanged across samples ($p > 0.05$), indicating minimal red-green variation. However, increasing pigface concentration significantly increased b* values ($p < 0.05$), confirming progressive yellowing associated with greater phenolic loading.

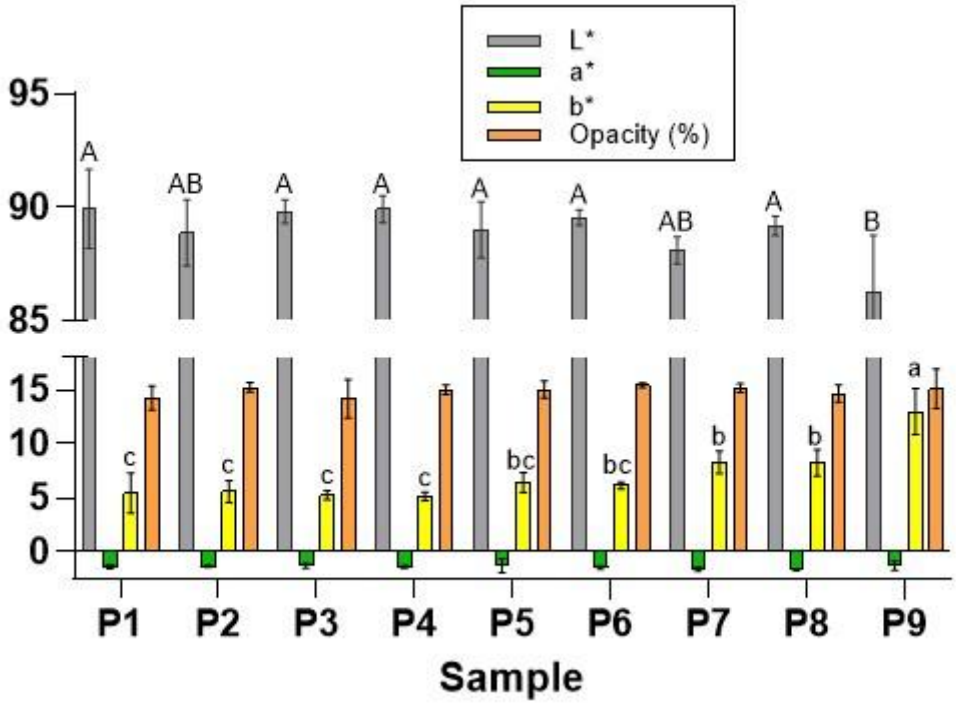


Fig. 5 Colour characteristics of agar-pigface films. Means within the same variable followed by different letters are significantly different (one-way ANOVA, $p < 0.05$). Uppercase letters denote differences in L; lowercase letters denote differences in b while opacity and a* values show no significant variation

Microstructural observations at 40× magnification (Supplementary Figure 1) showed clear morphology changes with increasing pigface incorporation. Film P1 (A:PF = 1:2.5) contained numerous voids (Supplementary Figure 1(a)), indicating a less compact matrix. In contrast, Film P6 (A:PF = 1:20) exhibited a tighter and more homogeneous structure (Supplementary Figure 1(b)), consistent with improved compatibility between pigface constituents and agar chains through intermolecular interactions. At higher extract loading (≥1:40, w/v), distinct agglomerates were visible within the film (Supplementary Figure 1(c)), which corresponded with the macroscopic loss of transparency observed in Figure 4(b). The overall miscibility and integration of pigface components within the agar matrix at intermediate loading are further illustrated in Figure 4(c) and Supplementary Figure 1(d). These agglomerates disrupt the agar network, lowering structural integrity and mechanical performance to 9.94 MPa tensile strength and 9.03% elongation at break. Similar trend was observed in the study on pea-starch film wherein excessive addition of apple polyphenols led to agglomeration within the matrix, that reduced the film's overall integrity [45]. Accordingly, an A:PF ratio of 1:20 delivered improved film characteristics without agglomeration.

3.2.3. Mechanical properties

Mechanical properties were evaluated through tensile strength (TS) and elongation at break (EAB), which are critical parameters for film performance [46, 47]. The agar control film exhibited limited mechanical performance, with a tensile strength of 15.81 ± 2.64 MPa and elongation at break of 11.95 ± 3.37%, reflecting its inherent brittleness. Film thickness ranged from 15.39 to 19.38 μm, with no significant differences among formulations ($p > 0.05$), indicating that mechanical variations were primarily attributable to compositional effects.

As shown in Figure 6(a), incorporation of pigface extracts significantly influenced mechanical behavior of films ($p<0.05$). Increasing the A:PF ratio from 1:10 to 1:20 (w/v) resulted in progressive improvements in both tensile strength and elongation. The highest tensile strength was observed at A:PF = 1:16 (P5), reaching 26.03 ± 6.47 MPa, while at A:PF = 1:20 (P6), tensile strength increased by approximately 38% relative to the control and

elongation at break increased by ~90% to 22-23%. These improvements corresponded with the compact microstructure observed in Supplementary Figure 1(b), suggesting enhanced intermolecular interactions within the matrix [48].

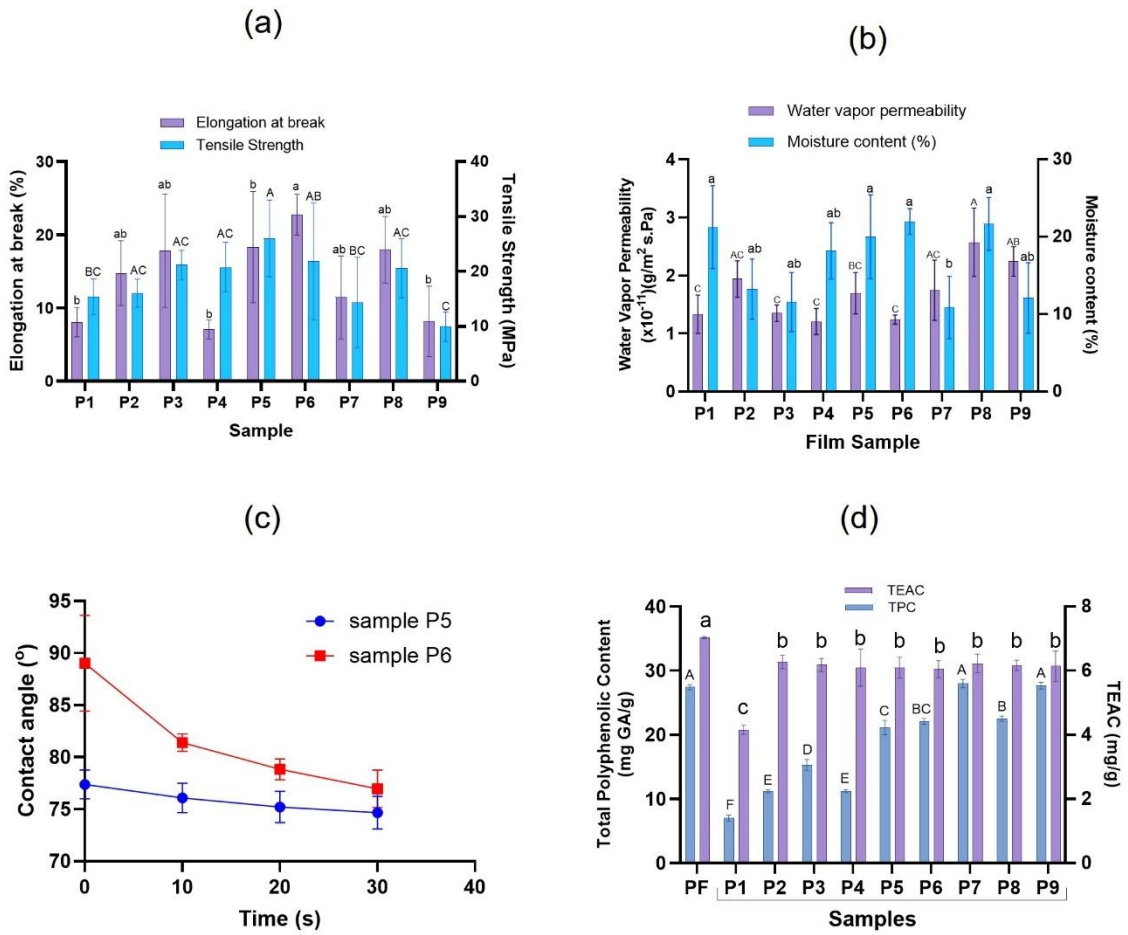


Fig. 6 Characterisation of agar-pigface (A:PF) composite films: (a) tensile strength (MPa) and elongation at break (%); (b) water vapour permeability and moisture content (%); (c) water contact angle (°) of P5 (A:PF 1:16) and P6 (A:PF 1:20); (d) antioxidant activity (total phenolic content, mg GAE/g, and TEAC, mg/g). Means within the same variable followed by different letters are significantly different (one-way ANOVA, $p < 0.05$)

At higher extract loading (A:PF = 1:40, w/v; P9), tensile strength decreased to 9.94 ± 2.7 MPa and elongation dropped below 9%, indicating a loss of structural integrity. This decline is attributed to excessive polyphenol incorporation, which disrupts polymer network continuity beyond an optimal threshold, consistent with observations in phenolic-modified biopolymer systems [49].

Elongation at break ranged from 7.05-22.77%, with maximum elongation observed at an A:PF ratio of 1:20 (w/v) (P6) (Figure 6(a)). The enhanced flexibility at intermediate pigface incorporation is consistent with the presence of low-molecular-weight carbohydrates and organic acids, including glucose, galactose, trehalose, and malic acid, identified by untargeted LC-MS analysis (Supplementary Table 4). According to Hou et al. [50] small molecules such as malic acid have been reported to exhibit plasticising effects in polymer systems by increasing chain mobility, which supports the observed increase in extensibility. These constituents likely contributed to internal plasticisation of the agar network at controlled concentrations. At lower A:PF ratios (e.g., 1:11), elongation at break decreased, which may be associated with increased agar concentration (2.2%), resulting in higher solution viscosity during casting and reduced molecular mobility within the dried matrix. At excessive pigface loading

(1:40, w/v; P9), elongation dropped below 9%, indicating brittle behaviour. This reduction is consistent with the agglomerate formation observed in Supplementary Figure 1(c), where phase discontinuities likely acted as stress concentration sites, reducing ductility. A similar concentration-dependent trend has been reported by Li et al. [45] wherein in polyphenol-modified biopolymer films improved the mechanical performance at moderate loading but declined beyond an optimal threshold due to aggregation effects.

Despite P6 exhibiting larger particle size (~1.45 μm) and a slightly higher ζ-potential magnitude (-18.2 mV) compared to P9 (~0.53 μm, -16.4 mV), it showed superior mechanical performance. This indicates that particle size alone does not determine mechanical strength; rather, dispersion quality and interfacial interactions are critical. Reduced ζ-potential magnitude in P9 suggests diminished electrostatic stability and increased aggregation, which disrupts load transfer within the matrix [51, 52]. In contrast, improved dispersion at intermediate concentrations promotes effective interaction between pigface-derived components and agar chains, resulting in a more cohesive network structure [53, 54]. Overall, the pigface extract acts as an active modifier rather than a passive filler. Within a defined compositional window, interactions between polyphenolic constituents and agar chains enhanced network cohesion, while low-molecular-weight carbohydrates and organic acids contributes to increased chain mobility, resulting in improved flexibility. These effects are consistent with changes in O-H stretching and C-O-C vibrations observed in FT-IR spectra, indicating modifications in the hydrogen bonding environment. At excessive loading, aggregation dominates, leading to structural discontinuities and brittle behaviour. This balance between interaction and aggregation defines a compositional window for optimal mechanical performance, distinguishing the composite from control agar films, which typically require external plasticisers to achieve comparable flexibility [47].

3.2.4. Moisture interaction and barrier properties

Moisture content (MC) of the films ranged from 10.87% to 21.97%. Lower MC values observed in P1 and P5 were associated with extended drying times required to obtain peelable films at lower solid contents. Film P7, containing a higher proportion of pigface extract (>46% (v/v)), exhibited significantly lower MC ($p < 0.05$), likely due to the formation of a more compact network structure that limited water retention. Similar behaviour has been reported in agar-based films incorporating plant extracts [55].

Water solubility ranged from 68.62 ± 4.13% to 99.7%. Except for P1, all films exhibited high solubility due to the hydrophilic nature of agar and the hydroxyl-rich pigface constituents. Although films initially retained structural integrity upon immersion, substantial degradation occurred after 24 h, indicating susceptibility to moisture-driven destabilisation [56].

The water vapour permeability (WVP), shown in Figure 6(b), measures the diffusing ability of water from the atmosphere passing through the film barrier to the contained product and a low WVP is desirable for preventing moisture absorption and extending product shelf life [57]. WVP performance decreased significantly ($p < 0.05$) as the A:PF ratio increased from 1:10 to 1:20 (w/v). The lowest WVP values were observed at 1:11 and 1:20, reaching 1.21×10^{-11} and 1.26×10^{-11} g/m²·s·Pa, respectively, compared with 2.91×10^{-11} g/m²·s·Pa for the control. This represents an approximate 57% reduction in permeability. The reduction is consistent with increased matrix compactness, which restricts water diffusion pathways and aligns with the data reported by Campa-Siqueiros et al. [58] where incorporating polyphenols of garlic extracts in agar film, exhibited a decline of WVP.

Contact angle measurements (Figure 6(c)) confirmed the hydrophilic nature of the films, with all values below 90° [59, 60]. Film P6 (A:PF 1:20, w/v) exhibited an approximately 16% higher initial contact angle than P5, suggesting slightly reduced surface wettability. For P6, the contact angle decreased from 89° to 81° within the first 10 s and further to 77° after 30 s, whereas P5 showed a more gradual decline from 77° to 75°. The higher initial contact angle for P6 is consistent with its denser microstructure, which may reduce immediate surface water penetration. However, the overall decrease in contact angle over time reflects the dominance of hydroxyl-rich constituents that promote water interaction.

Comparable contact angle ranges have been reported by Guo et al. [61] in agar-starch composite films (59.72 ± 3.82° to 78.34 ± 3.0°), with higher values observed only in formulations exhibiting increased surface roughness.

Similarly, agar films incorporating 2.5-10% nanocellulose showed contact angles between 60.83 ± 0.33° and 65.58 ± 1.18° [44]. These comparisons indicate that the wettability behaviour of the pigface-agar films is consistent with other hydrophilic polysaccharide-based systems.

3.2.5. Antioxidant activity

The antioxidant activity of the agar-pigface composite films was evaluated through total phenolic content (TPC), DPPH radical scavenging activity, and Trolox Equivalent Antioxidant Capacity (TEAC), as presented in Figure 6(d) and serve a crucial role as radical scavengers due to their active components in biodegradable packaging [62]. The agar control exhibited minimal antioxidant activity, with a TPC of 2.47 ± 0.14 mg GAE/100 g (Supplementary Table 5), confirming that antioxidant functionality was derived primarily from pigface incorporation.

TPC increased significantly with increasing pigface concentration ($p < 0.05$), ranging from 7.0 ± 0.47 to 28.0 ± 0.65 mg GAE/g. DPPH scavenging activity increased from 48% in the lowest pigface formulation (A:PF = 1:2.5, w/v) to 73.4-77.2% in higher-loading films. Similarly, TEAC values increased from 4.16 mg Trolox/g to 6.05-6.28 mg Trolox/g. These results demonstrate a clear concentration-dependent relationship between phenolic incorporation and antioxidant capacity. Compared with previously reported agar-based films, the pigface-enriched formulations exhibited substantially higher phenolic content. For example, agar films containing 5% *Hibiscus sabdariffa* seed extract showed TPC values of 0.64 mg GAE/100 g, while films containing 1-2% mushroom powder exhibited 0.90-1.89 mg GAE/100 g [41].

LC-MS analysis identified catechin, (+)-gallocatechin, taxifolin, salicylic acid, neochlorogenic acid, and ferulic acid as predominant constituents within the extract. The phenolic hydroxyl groups of these compounds facilitate hydrogen atom donation and electron transfer, supporting the observed radical scavenging activity [63]. Overall, antioxidant activity was retained after film formation and scaled proportionally with pigface concentration, indicating that the bioactive compounds remained functionally stable within the agar matrix.

4. Conclusion and future recommendations

Pigface (Carpobrotus glaucescens) leaf extract was characterised as a polyphenol- and carbohydrate-rich matrix with abundant hydroxylated and glycosylated metabolites, which supports the hypothesis that these constituents can interact with agar chains and act as internal plasticising agents. When incorporated into agar, the extract functioned as a structurally interactive modifier rather than a passive additive. At an agar-to-pigface ratio of 1:20 (w/v), tensile strength increased by approximately 38%, elongation at break by approximately 90%, and water vapour permeability decreased by approximately 57% relative to the control. These improvements are consistent with a combined effect of network reinforcement through polyphenol-agar interactions and internal plasticisation by low-molecular-weight constituents, mitigating the inherent brittleness of agar films while introducing antioxidant functionality.

At higher extract concentrations, particle aggregation disrupted matrix continuity and reduced mechanical performance, indicating a defined optimal compositional range. Despite improved mechanical and barrier properties, the films remained highly water-soluble, limiting their suitability for moisture-rich environments. In addition, the presence of elevated arsenic levels in raw pigface highlights the importance of controlled sourcing and contaminant management in plant derived materials.

Overall, this study demonstrates that complex phytochemical mixtures can modulate the behaviour of biodegradable polymer systems in a concentration-dependent manner. These findings provide a basis for designing bio-based polymer materials with tunable structure-property relationships through controlled incorporation of chemically diverse natural modifiers. Future work should focus on improving water resistance and evaluating long-term stability and safety for potential applications.

5. Acknowledgements

Amino acid analyses were performed using NCRIS-enabled infrastructure at the Australian Proteome Analysis Facility (APAF). LC-MS, NMR, and CHNS elemental analyses were conducted at the UNSW Mark Wainwright Analytical Centre (MWAC). We acknowledge IndigiGrow for providing plant materials and for their community partnership. The idea to explore native ingredients in functional materials was inspired by the brilliant keynote speech of Mindy Woods, a proud Bundjalung woman and founder of Karkalla, at For Food's Sake 2025 in Coffs Harbour (Gumbaynggirr Country), hosted by Future Food Systems CRC. The authors also acknowledge the financial support provided through UNSW Societal Impact Seed Funding as well as the guidance throughout the project from Prof. Greg Leslie (UNSW School of Chemical Engineering), Prof. Daniel Robinson (UNSW School of Arts, Design and Architecture), Dr. Eva Lloyd (UNSW School of Built Environment), and Mr. Phil Pettitt (Community Greening Manager- Royal Botanic Gardens, Sydney).

6. Author contributions

Rishi Ravindra Naik: Conceptualization, Methodology, Investigation, Resources, Data curation, Writing – original draft, Writing – review & editing, Visualization, Funding acquisition, Supervision, Project administration; **Que Trinh Tran:** Investigation, Data curation, Writing – original draft, Writing – review & editing, Visualization; **Muhammad Bin Zia:** Investigation, Visualization, Writing – review & editing; **Cordelia Selomulya:** Conceptualization, Resources, Writing – review & editing, Supervision, Project administration, Funding acquisition. All authors have read and approved the final manuscript and agree to be accountable for all aspects of the work.

7. Declaration of competing interest

The authors declare that they have no known competing financial interests or personal relationships that could have appeared to influence the work reported in this paper.

8. Funding Declaration

The authors acknowledge the financial support provided through UNSW Societal Impact Seed grant 2025.

9. References

1. Mostafavi FS, Zaeim D (2020) Agar-based edible films for food packaging applications-A review. International journal of biological macromolecules.159:1165-76.

2. Ritchie H, Samborska, V. and Roser, M. : Plastic pollution, Our World in Data. . https://ourworldindata.org/plastic-pollution (2023). Accessed 11 March 2026.

3. Ammendolia J, Walker TR (2022) Citizen science: A way forward in tackling the plastic pollution crisis during and beyond the COVID-19 pandemic. Science of The Total Environment.805:149957. doi: https://doi.org/10.1016/j.scitotenv.2021.149957 .

4. Misgana B, Tucho GT (2022) Assessment of Community's Perception Toward Single-Use Plastic Shopping Bags and Use of Alternative Bags in Jimma Town, Ethiopia. Environ Health Insights.16:11786302221085047. doi: https://doi.org/10.1177/11786302221085047 .

5. Petaloti A-I, Makri S, Achilias DS (2024) Bioactive edible gel films based on wheat flour and glucose for food packaging applications. Gels.10(2):105.

6. Giosafatto CVL, Di Pierro P, Gunning AP, Mackie A, Porta R, Mariniello L (2014) Trehalose-containing hydrocolloid edible films prepared in the presence of transglutaminase. Biopolymers.101(9):931-7.

7. Karsten U, Görs S, Eggert A, West JA (2007) Trehalose, digeneaside, and floridoside in the Florideophyceae (Rhodophyta)-a reevaluation of its chemotaxonomic value. Phycologia.46(2):143-50.

8. Li H, Gao Z, Zhang X, Li Z, Meng L, Li S, et al. (2025) Polysaccharide-based edible films loaded with bioactive components for food applications: A review. International Journal of Biological Macromolecules.147589.

9. Patel N, Bagul H, Krishnamurthy R. Cultural Perspectives on Edible Plants. The Future of Food: Exploring Edible Plants for a Sustainable Diet. Springer; 2026. p. 103-15.

10. Dipu MA, Checco J, Williams L, Sultanbawa Y, Jones NA, Aziz AA (2025) Navigating challenges in native plant-based food value chains within the global food system: A systematic literature review. Agricultural Systems.228:104373.

11. Martín-Forés I, Guerin GR, Lewis D, Gallagher RV, Vilà M, Catford JA, et al. (2024) Towards integrating and harmonising information on plant invasions across Australia. NeoBiota.92:61-83.

12. Hardwick P (2023) REPORT: Non-native *Carpobrotus* risk to native *Carpobrotus glaucescens* from hybridisation and invasiveness.

13. Earnshaw M, Carver K, Charlton W (1987) Leaf anatomy, water relations and crassulacean acid metabolism in the chlorenchyma and colourless internal water-storage tissue of *Carpobrotus edulis* and *Senecio*? mandraliscae. Planta.170(3):421-32.

14. ElementarAnalysensysteme_GmbH. Operating instructions vario MACRO cube CHNOS Elemental Analyzer. In: Langenselbold GEAG, editor. Germany: Elementar Analysensysteme GmbH.; 2017.

15. Bosch L, Alegría A, Farré R (2006) Application of the 6-aminoquinolyl-N-hydroxysccinimidyl carbamate (AQC) reagent to the RP-HPLC determination of amino acids in infant foods. Journal of Chromatography B.831(1):176-83. doi: https://doi.org/10.1016/j.jchromb.2005.12.002 .

16. Cohen SA. Amino Acid Analysis Using Precolumn Derivatization with 6-Aminoquinolyl-N-Hydroxysuccinimidyl Carbamate. In: Cooper C, Packer N, Williams K, editors. Amino Acid Analysis Protocols. Totowa, NJ: Humana Press; 2000. p. 39-47.

17. Cohen SA, De Antonis KM (1994) Applications of amino acid derivatization with 6-aminoquinolyl-N-hydroxysuccinimidyl carbamate: Analysis of feed grains, intravenous solutions and glycoproteins. Journal of Chromatography A.661(1):25-34. doi: https://doi.org/10.1016/0021-9673(93)E0821-B .

18. Cohen SA, Michaud DP (1993) Synthesis of a Fluorescent Derivatizing Reagent, 6-Aminoquinolyl-N-Hydroxysuccinimidyl Carbamate, and Its Application for the Analysis of Hydrolysate Amino Acids via High-Performance Liquid Chromatography. Analytical Biochemistry.211(2):279-87. doi: https://doi.org/10.1006/abio.1993.1270 .

19. Lv P, Ye Q, Wang Y, Mao L, Yu R, Selomulya C (2025) Rice protein-based gel particles for Pickering emulsion. Food Hydrocolloids.169:111655.

20. Kim HK, Choi YH, Verpoorte R (2010) NMR-based metabolomic analysis of plants. Nature protocols.5(3):536-49.

21. Link DD, Walter PJ, Kingston HM (1998) Development and Validation of the New EPA Microwave-Assisted Leach Method 3051A. Environmental Science & Technology.32(22):3628-32. doi: https://doi.org/10.1021/es980559n .

22. Bobo-García G, Davidov-Pardo G, Arroqui C, Vírseda P, Marín-Arroyo MR, Navarro M (2015) Intra-laboratory validation of microplate methods for total phenolic content and antioxidant activity on polyphenolic extracts, and comparison with conventional spectrophotometric methods. Journal of the Science of Food and Agriculture.95(1):204-9.

547 23. Sari KRP, Ikawati Z, Danarti R, Hertiani T (2023) Micro-titer plate assay for measurement of total phenolic
548 and total flavonoid contents in medicinal plant extracts. Arabian Journal of Chemistry.16(9):105003.

549 24. Martínez-Sanz M, Gómez-Mascaraque LG, Ballester AR, Martínez-Abad A, Brodkorb A, López-Rubio A
550 (2019) Production of unpurified agar-based extracts from red seaweed Gelidium sesquipedale by means of
551 simplified extraction protocols. Algal Research.38:101420. doi: https://doi.org/10.1016/j.algal.2019.101420 .

552 25. Ermi Hikmawanti NP, Fatmawati S, Asri AW. The effect of ethanol concentrations as the extraction solvent
553 on antioxidant activity of Katuk (Sauropus androgynus (L.) Merr.) leaves extracts. IOP conference series: Earth
554 and environmental science: IOP Publishing; 2021. p. 012060.

555 26. Test Method for Tensile Properties of Thin Plastic Sheeting. ASTM International.

556 27. Homez-Jara A, Daza LD, Aguirre DM, Muñoz JA, Solanilla JF, Váquiro HA (2018) Characterization of
557 chitosan edible films obtained with various polymer concentrations and drying temperatures. International
558 journal of biological macromolecules.113:1233-40.

559 28. Sutharsan J, Boyer CA, Zhao J (2022) Physicochemical properties of chitosan edible films incorporated with
560 different classes of flavonoids. Carbohydrate Polymer Technologies and Applications.4:100232.

561 29. Makhloufi N, Chougui N, Rezgui F, Benramdane E, Silvestre AJ, Freire CS, et al. (2022) Polysaccharide-
562 based films of cactus mucilage and agar with antioxidant properties for active food packaging. Polym
563 Bull.79(12):11369-88.

564 30. Sun Y, Guo J, Li Y, Luo G, Li L, Yuan H, et al. (2020) Negative effects of the simulated nitrogen deposition
565 on plant phenolic metabolism: A meta-analysis. Science of the Total Environment.719:137442.

566 31. Alisi C, Bacchetta L, Bojorquez E, Falconieri M, Gagliardi S, Insaurralde M, et al. (2021) Mucilages from
567 different plant species affect the characteristics of bio-mortars for restoration. Coatings.11(1):75.

568 32. Nandiyanto ABD, Oktiani R, Ragadhita R (2019) How to read and interpret FTIR spectroscope of organic
569 material. Indonesian Journal of Science and Technology.4(1):97-118.

570 33. Liu X: 1H NMR spectra and interpretation (part I), .
571 https://chem.libretexts.org/Bookshelves/Organic_Chemistry/Organic_Chemistry_I_(Liu)/06%3A_Structural_Id
572 entification_of_Organic_Compounds-
573 _IR_and_NMR_Spectroscopy/6.06%3A_H_NMR_Spectra_and_Interpretation_(Part_I) (2021). Accessed 01
574 February 2026.

575 34. Lyubchyk S, Shapovalova O, Lygina O, Oliveira MC, Appazov N, Lyubchyk A, et al. (2019) Integrated
576 Green Chemical Approach to the Medicinal Plant *Carpobrotus edulis* Processing. Scientific Reports.9(1):18171.
577 doi: https://doi.org/10.1038/s41598-019-53817-8 .

578 35. Codex(CXS193-1995): Codex Alimentarius Commission, General Standard for Contaminants and Toxins in
579 Food and Feed (CXS 193-1995). https://www.fao.org/fao-who-codexalimentarius/codex-texts/list-standards/en/
580 (2024). Accessed 8 March 2025.

581 36. Shahid M, Dumat C, Khalid S, Schreck E, Xiong T, Niazi NK (2017) Foliar heavy metal uptake, toxicity
582 and detoxification in plants: A comparison of foliar and root metal uptake. J Hazard Mater.325:36-58. doi:
583 https://doi.org/10.1016/j.jhazmat.2016.11.063.

584 37. Patel M, Parida AK (2023) Salinity alleviates arsenic stress-induced oxidative damage via antioxidative
585 defense and metabolic adjustment in the root of the halophyte Salvadora persica. Planta.258(6):109. doi:
586 https://doi.org/10.1007/s00425-023-04263-4 .

587 38. Akinyede KA, Ekpo OE, Oguntibeju OO (2020) Ethnopharmacology, therapeutic properties and nutritional
588 potentials of *Carpobrotus edulis*: A comprehensive review. Sci Pharm.88(3):39.

589 39. Shahidi F, Athiyappan KD (2025) Polyphenol-polysaccharide interactions: molecular mechanisms and
590 potential applications in food systems - a comprehensive review. Food Production, Processing and
591 Nutrition.7(1):42. doi: https://doi.org/10.1186/s43014-025-00322-3 .

592 40. Dordevic S, Dordevic D, Sedlacek P, Kalina M, Tesikova K, Antonic B, et al. (2021) Incorporation of
593 Natural Blueberry, Red Grapes and Parsley Extract By-Products into the Production of Chitosan Edible Films.
594 Polymers.13(19):3388.

595 41. de Oliveira Dias J, de Carvalho RA, Nunes A, dos Santos Garcia RH, de Menezes Rodrigues G, Yoshida
596 CMP, et al. (2025) Oral disintegration films based on agar-agar with incorporation of hydroalcoholic extract of
597 Hibiscus sabdariffa seeds. International Journal of Biological Macromolecules.330:147984. doi:
598 https://doi.org/10.1016/j.ijbiomac.2025.147984 .

599 42. Wang L, Dong Y, Men H, Tong J, Zhou J (2013) Preparation and characterization of active films based on
600 chitosan incorporated tea polyphenols. Food Hydrocolloids.32(1):35-41. doi:
601 https://doi.org/10.1016/j.foodhyd.2012.11.034 .

602 43. Sun L, Sun J, Chen L, Niu P, Yang X, Guo Y (2017) Preparation and characterization of chitosan film
603 incorporated with thinned young apple polyphenols as an active packaging material. Carbohydrate
604 Polymers.163:81-91. doi: https://doi.org/10.1016/j.carbpol.2017.01.016 .

605 44. Atef M, Rezaei M, Behrooz R (2014) Preparation and characterization agar-based nanocomposite film
606 reinforced by nanocrystalline cellulose. International journal of biological macromolecules.70:537-44.

607 45. Li X, Liu Y, Luo B, Xiang W, Chen Z (2024) Effect of apple polyphenols on physicochemical properties of
608 pea starch/pulp cellulose nanofiber composite biodegradable films. International Journal of Biological
609 Macromolecules.257:128480. doi: https://doi.org/10.1016/j.ijbiomac.2023.128480 .

610 46. Shah YA, Bhatia S, Al-Harrasi A, Afzaal M, Saeed F, Anwer MK, et al. (2023) Mechanical Properties of
611 Protein-Based Food Packaging Materials. Polymers.15(7):1724.

612 47. Fang Y, Tung M, Britt I, Yada S, Dalgleish D (2002) Tensile and barrier properties of edible films made
613 from whey proteins. Journal of Food Science.67(1):188-93.

614 48. Hamed YS, Hassan KR, Ahsan HM, Hussain M, Wang J, Zou X-G, et al. (2024) Development of chitosan-
615 based edible film incorporated with purified flavonoids from Moringa oleifera: Structural, thermal, antibacterial
616 activity and application. Food chemistry.457:140059.

617 49. Orliac O, Rouilly A, Silvestre F, Rigal L (2002) Effects of additives on the mechanical properties,
618 hydrophobicity and water uptake of thermo-moulded films produced from sunflower protein isolate.
619 Polymer.43(20):5417-25.

620 50. Hou B, Sun Y, Guo Y, Zhang W, Shan X, Cui Q, et al. (2024) Synthesis, characterization, and performance
621 evaluation of a high-efficiency fully biobased biodegradable plasticizer. Journal of Applied Polymer
622 Science.141(45):e56225.

623 51. Giménez B, De Lacey AL, Pérez-Santín E, López-Caballero M, Montero P (2013) Release of active
624 compounds from agar and agar-gelatin films with green tea extract. Food Hydrocolloids.30(1):264-71.

625 52. De Paola MG, Paletta R, Lopresto CG, Lio GE, De Luca A, Chakraborty S, et al. (2021) Stability of film-
626 forming dispersions: Affects the morphology and optical properties of polymeric films. Polymers.13(9):1464.

627 53. Boey JY, Lee CK, Tay GS (2022) Factors affecting mechanical properties of reinforced bioplastics: a
628 review. Polymers.14(18):3737.

629 54. Prateepchanachai S, Thakhiew W, Devahastin S, Soponronnarit S (2017) Mechanical properties
630 improvement of chitosan films via the use of plasticizer, charge modifying agent and film solution
631 homogenization. Carbohydrate Polymers.174:253-61.

632 55. Kanmani P, Rhim J-W (2014) Antimicrobial and physical-mechanical properties of agar-based films
633 incorporated with grapefruit seed extract. Carbohydrate polymers.102:708-16.

634 56. Rachtanapun P, Tongdeesoontorn W (2009) Effect of antioxidants on properties of rice flour/cassava starch
635 film blends plasticized with sorbitol. Agriculture and Natural Resources.43(5):252-8.

636 57. Saidi L, Wang Y, Wich PR, Selomulya C (2025) Polysaccharide-based edible films-strategies to minimize
637 water vapor permeability. Current Opinion in Food Science.61:101258.

638 58. Campa-Siqueiros PI, Vargas-Arispuro I, Quintana-Owen P, Freile-Pelegrín Y, Azamar-Barrios JA, Madera-
639 Santana TJ (2020) Physicochemical and transport properties of biodegradable agar films impregnated with
640 natural semiochemical based-on hydroalcoholic garlic extract. International Journal of Biological
641 Macromolecules.151:27-35.

642 59. Jhaveri JH, Murthy Z (2016) A comprehensive review on anti-fouling nanocomposite membranes for
643 pressure driven membrane separation processes. Desalination.379:137-54.

644 60. Phan TD, Debeaufort F, Luu D, Voilley A (2005) Functional Properties of Edible Agar-Based and Starch-
645 Based Films for Food Quality Preservation. Journal of Agricultural and Food Chemistry.53(4):973-81. doi:
646 https://doi.org/10.1021/jf040309s .

647 61. Guo Y, Zhang B, Zhao S, Qiao D, Xie F (2021) Plasticized starch/agar composite films: Processing,
648 morphology, structure, mechanical properties and surface hydrophilicity. Coatings.11(3):311.

649 62. Gómez-Estaca J, López-de-Dicastillo C, Hernández-Muñoz P, Catalá R, Gavara R (2014) Advances in
650 antioxidant active food packaging. Trends in Food Science & Technology.35(1):42-51.

651 63. Abd El-Hack ME, de Oliveira MC, Attia YA, Kamal M, Almohmadi NH, Youssef IM, et al. (2023) The
652 efficacy of polyphenols as an antioxidant agent: An updated review. International Journal of Biological
653 Macromolecules.250:126525.

654 64. Broomhead NK, Moodley R, Jonnalagadda SB (2020) Chemical and elemental analysis of the edible fruit of
655 five *Carpobrotus species* from South Africa: Assessment of nutritional value and potential metal toxicity.
656 International Journal of Environmental Health Research.30(4):357-71.

657 65. Wuana RA, Okieimen FE (2011) Heavy metals in contaminated soils: a review of sources, chemistry, risks
658 and best available strategies for remediation. International Scholarly Research Notices.2011(1):402647.

659 66. Seo YJ (2013) NMR - Interpretation. Chemistry LibreTexts

660

Supplementary Files

This is a list of supplementary files associated with this preprint. Click to download.

- Supplementaryinformation.docx